Journal of Power Sources 641 (2025) 236723

Contents lists available at ScienceDirect

Journal of Power Sources

journal homepage: www.elsevier.com/locate/jpowsour

A photovoltaics emulator for electrochemistry using Python and SCPI

Martin Florian Seidler [a,b,*], Bart Pieters [a], Walter Zwaygardt [b], Stefan Haas [a], Oleksandr Astakhov [a], Tsvetelina Merdzhanova [a]

[a] IEK-5 Photovoltaics at Forschungszentrum Jülich GmbH, 52425, Jülich, Germany
[b] IEK-14 Electrochemical Process Engineering at Forschungszentrum Jülich GmbH, 52425, Jülich, Germany

HIGHLIGHTS

- Photovoltaics emulators provide weather independence and output scalability.
- Our software focused emulator offers high accuracy and reproducibility.
- We improved convergence and reduced ripple for electrochemical devices.
- We show reliability and 1 s response time in two 24 h validation runs.
- The emulator consists of off the shelf hardware and free and open source software.

GRAPHICAL ABSTRACT

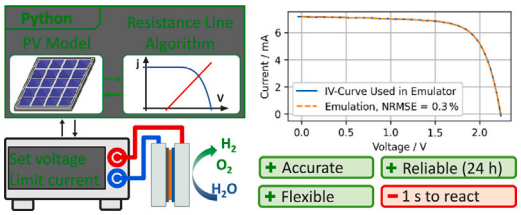

ARTICLE INFO

Keywords:
Photovoltaics
Emulator
Power supply
Electrolysis
Python
SCPI

ABSTRACT

Coupling photovoltaics to electrochemical devices is one of the major routes to overcome intermittent power generation and facilitate further PV deployment. However, for practical tests researchers are often at the whims of the environmental conditions at their testing sites. Experimental devices may be constrained to laboratory environments, which makes coupling to physical photovoltaics impractical. To avoid these limitations, photovoltaic devices can be emulated using highly specialized custom hardware. Adding to this development, we show emulation in software using only common functions available in many off the shelf laboratory power supplies. This approach offers maximum flexibility in choosing a photovoltaic model and operating conditions, both of which may be measured, predicted or entirely artificial. It is geared towards electrochemistry updating the output 2 times per second typically and reproducing the current–voltage characteristics of the photovoltaic device with high accuracy (0.3 % error). It also provides fast convergence for electrochemical loads and protects them from excessive ripple currents.

1. Introduction

Storage of electrical energy generated by photovoltaics (PV) is one of the key issues in the global transition to green energy [1,2]. The intermittent PV generation requires particularly long-term energy storage. Electrochemical devices are expected to back PV up by producing carbon free fuel (water electrolysis) [3–6] or sinking CO_2 into other useful chemicals (electrochemical CO_2 reduction) [7–11].

These electrochemical devices however perform best under constant power and may suffer performance loss and early failure due to accelerated degradation under significant power fluctuations [12–14]. Achieving a good capacity factor and longevity in electrolyzer devices is the major challenge in coupling to PVs which are naturally intermittent due to diurnal cycles, seasonality and environmental conditions. Therefore measuring the effects which these fluctuations in power

* Correspondence to: 52425 Jülich, Germany.
E-mail addresses: f.seidler@fz-juelich.de (M.F. Seidler), b.pieters@fz-juelich.de (B. Pieters), w.zwaygardt@fz-juelich.de (W. Zwaygardt), st.haas@fz-juelich.de (S. Haas), o.astakhov@fz-juelich.de (O. Astakhov), t.merdzhanova@fz-juelich.de (T. Merdzhanova).

https://doi.org/10.1016/j.jpowsour.2025.236723
Received 12 July 2024; Received in revised form 28 February 2025; Accepted 3 March 2025
Available online 20 March 2025

supply have on electrochemical devices is essential for evaluating their dynamic performance and wear.

While it is possible to perform such tests using a physical PV device connected to an electrolyzer, emulation of the PV device offers much greater flexibility. An adequate PV-emulation device offers the possibility to test an arbitrary time-series of conditions, with arbitrary PV devices, in a reproducible manner within a laboratory. This way, standard reproducible tests can be performed to ensure comparability of results from electrochemical devices. The versatility of this approach motivates development of various PV emulators, e.g. [15,16], including some large scale commercially available solutions, e.g. [17–19]. They are, however, not common equipment in electrochemistry labs due to their highly specialized nature. In this work we describe a software focused approach to realizing a PV emulator with off-the-shelf components which should be readily available in a typical electrochemistry laboratory.

We built the emulator described here to accurately replicate the behavior of a photovoltaic cell or module under various operating conditions. In other words the emulator is developed to reproduce any required IV characteristic of a PV device. For example, researchers may want to study direct coupling of an experimental PV-module (V_{OC} =56 V) to an also experimental electrochemical cell. However, a single laboratory scale (e.g. 5 cm^2) water electrolysis cell is severely mismatched, especially in terms of voltage. In this case, either a specialized PV module must be developed, or the electrolyzer cell must be upscaled and stacked, or both, to match the IV characteristics of both devices. These "fine-tuning" adjustments are very challenging tasks performed by different research groups over long periods of time and can only cover one specific combination. Alternatively, the researchers would have to acquire a specialized hardware emulator with matching electrical characteristics, the ability to scale the output current and voltage, and to be programmable with specific, publicly not yet available module characteristics. If they scale up to larger cells or stacks they likely need another emulator device. The free and open source software (FOSS) based emulator presented in this article can solve all these issues and more. Any complex scenario of irradiance and temperature for the PV module over the required time frame can be accurately replicated the required number of times, facilitating detailed and reproducible comparison of different electrochemical devices under realistic conditions. The proposed emulation can interface with already available devices at various electrical power scales and take the required scaling and modeling inputs. In contrast to proprietary code on commercial emulators it can be adapted without restriction. For example, our code (in supplement) provides emulation of typical IV-curves. If a study requires emulation of more specific effects, such as shadowing or degradation, the model or time series to describe these effects, be it measured or generated, must be developed by the researchers conducting that study. For compatibility with our code the addition needs to provide either IV-curves or IEC60891:2021 compatible parameters and the `fobj` callable object (defined at line 46 interpolation version, at line 161 IEC norm version) needs to be updated in the main control loop update section (starting from line 200 interpolation version, starting from line 227 IEC norm version). Therein lies the unique flexibility and the novelty of our approach. Accuracy can be best in class when using appropriate hardware. The only significant limitation is the slow reaction time of 1 s.

The commercial solutions [17–19] offer similar input features as our software for data input (IV-curves, operating conditions), but start at a power of 2 kW, which is not suitable for experiments with single cells. However, they claim maximum power point tracking capability, which our approach cannot offer due to its slow reaction time. To the best of our knowledge no other FOSS besides our PV emulator is available at the time of writing.

Methods (Section 2) describes the algorithm used for tracking the correct working point and the PV models we used with the emulator. We then evaluate the emulator's capabilities in Section 3 followed by a discussion of the performance we found in Section 4. We conclude with Section 5 remarking on the capabilities and potential applications of the emulator.

2. Methods

Our goal in choosing the components for the emulator was to ensure flexibility and accessibility. Therefore, we chose the Keithley 2460 SMU (source measure unit) [20]. It offers a wide array of connectivity (Ethernet, USB, GPIB and TSP-Link). It also uses the SCPI (Standard Commands for Programmable Instruments [21]) command set which is common in laboratory bench top devices. The emulation is implemented using a Python script which controls the SMU output (script in supplementary information). The gap between the high-level, open-source Python and the hardware interface of the SMU is bridged by the National Instruments VISA library in conjunction with the PyVisa package. Although VISA is not open source, it is freely available [22] and the Windows operating system was chosen for its ubiquity (however we expect that the developed solution will be functional on other platforms, e.g. Linux).

The versatility and use of typical electrochemical lab components comes at the cost of bandwidth. The emulator has much smaller bandwidth than the physical device, i.e. the emulator updates the output at a minimum time step of 0.5 s while a physical PV module typically takes 0.1 ms to 10 ms to settle (within 10 %) after a step change in irradiance [23]. This fortunately has little impact on the use of the emulator to replicate the power output of a typical terrestrial PV installation, e.g. over one day. Frequency analysis of such measurements shows no significant contributions above 0.1 Hz (see e.g. [24]) requiring a settling time of ≤5 s.

2.1. Resistance line algorithm

The algorithm at the heart of the Python script (see supplemental) is inspired by [16]. We have implemented it by using the ability of the SMU to measure and report back current and voltage while setting a maximum output voltage and limiting current, i.e. working as a current-limited voltage source. The emulator can be used in two-wire or four-wire mode to minimize the impact of wire resistances.

The working principle of the algorithm is depicted in Fig. 1: As an input the emulator takes a current–voltage-curve (IV-curve) of the device it will emulate in tabular form. The IV-curve is analyzed and three key quantities are determined: open circuit voltage V_{oc}, voltage at the maximum power point V_{mpp} and current at the maximum power point I_{mpp}. The emulator starts with a default assumption for the load resistance of $R_0 = V_{mpp}/I_{mpp}$ (the so-called characteristic resistance of a PV device). Initially the output voltage is set to the open circuit voltage V_{oc} of the emulated PV device and the current is limited to $I_{lim} = I_{mpp}$ (Fig. 1 A). The program then immediately continues by starting the control loop.

At the start of the first control loop cycle the emulator measures the load voltage and current under the initial conditions. Depending on the load this could be either $V_l = V_{oc}$ and $I_l \leq I_{mpp}$ or $V_l < V_{oc}$ and $I_l = I_{mpp}$. We refer to this point in the IV plot as the working point (WP in Fig. 1 B). From Ohm's law the program finds an estimate of the load resistance $R_l = V_l/I_l$. Based on this estimate, the program finds the intersection of the IV-curve of the PV device $I_{PV}(V)$ and the linear function given by $I_R(V) = 1/R_l \cdot V_l$ (IP in Fig. 1 C). This function is also called the resistance line (R in Fig. 1 A), giving the resistance line method described here its name.

Finding this intersection is equivalent to finding the root of $I_{PV}(V) = I_R(V)$. This task is fulfilled by the function "optimize.root_scalar" from the Python package SciPy [25]. For root-finding, the IV-curve which consists of a finite amount of measurements is interpolated linearly, i.e. the program also finds intersection points between input voltages. Then the current limit is set according to this intersection point and the program waits just long enough for a full time step (e.g. 0.5 s) to complete.

In general the load is not an ohmic resistor as it is the case with electrochemical devices. Therefore, the load will settle in a new working

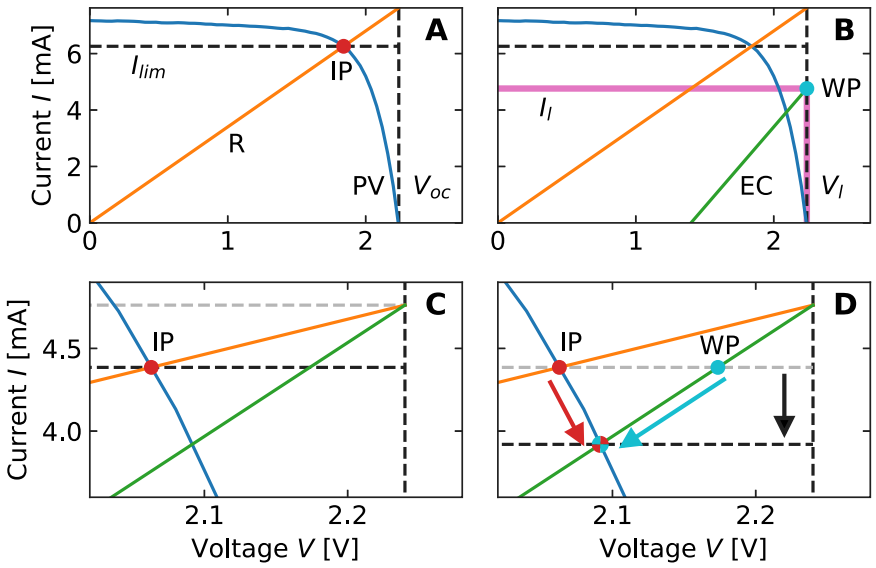

Fig. 1. A: The initial guess for load resistance is made such that the line representing it (labeled R) has its intersection point (IP) with the PV cell current–voltage-curve at the maximum power point. B: After activating supply the load (EC) settles at the working point (WP) with voltage V_l and current I_l, in this case $V_l = V_{oc}$ and $I_l < I_{lim}$. C: The estimation for load resistance is updated to reflect the working point. A new, in this example lower, current limit is set based on the intersection of resistor line and PV curve. D: Repeating steps B-C, working point and intersection point converge at the intersection point of load line and PV curve.

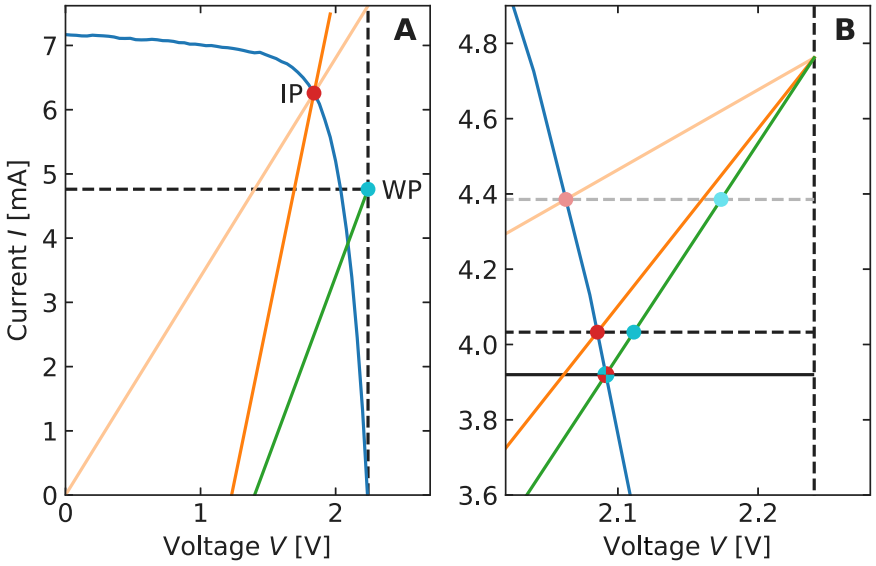

Fig. 2. Faster convergence with offset voltage. A: Initial guess (IP) and first working point (WP). Lighter colors show the process without offset. Offset value is 1.23 V. B: With the offset, after the first iteration the emulator is 4x closer to the final, correct current limit (black solid line) than without offset.

point closer to, but not on the IV-curve (WP in Fig. 1 D). In response, the resistance estimation and current limit will be adjusted by repeating the previous steps (B and C) to minimize the deviation between calculated intersection and measured working point. Therefore, the working point is effectively moved onto and kept on the IV-curve of the emulated PV device.

We develop this emulator mostly for electrochemical loads and therefore made two special adaptations to the algorithm. First: we can roughly approximate most electrolyzers' non-linear IV-curve with a linear IV-curve originating at a certain offset voltage V_o so that $I(V_{ec}) \approx (V_{ec} - V_o)/R_{ec}$, while $I(V_{ec}) = 0$ for $V_{ec} < V_o$. We use this approximation by estimating the load resistance (step B) as $R_l = (V_l - V_o)/I_l$. It follows that the program needs to calculate the resistance line (step C) as $I_R(V) = \cdot(V_l - V_o)/R_l$. To avoid causing division by zero we choose the voltage V_o lower than would usually be considered the best fit. For example for water electrolysis the thermoneutral voltage of 1.48 V at standard conditions would fit well. However, using the reversible voltage of 1.23 V at standard conditions already speeds up convergence as depicted in Fig. 2 and significantly reduces the risk of encountering divide by zero errors.

The second addition is a so called "dead zone" the tolerance within which no adjustment is needed. It is a range of resistances around the currently set one. As long as measured load resistance stays within this range no control action is applied, i.e. no change in current limit. This feature avoids ripple currents which are suspected to induce additional degradation in electrolyzers [12].

2.2. PV model and inclusion of operating conditions

If the goal is to operate following a fixed IV-curve, the emulator program can be used in this way and requires just the one IV-curve. However, if more data are available it can take temperature and

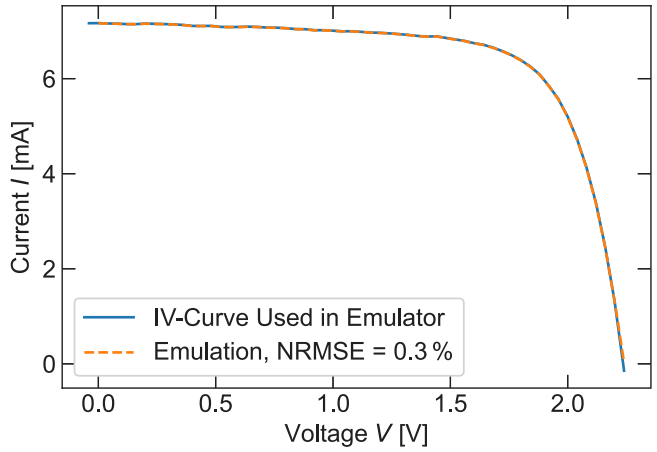

Fig. 3. Comparison between a solar cell measurement and its emulation. The output of the emulator was tested on an AM1.5G class-A sun simulator from Wacom, only using the electronic load component which usually measures current at increasing voltages across PV module terminals. Each point was sampled for 1 s. The emulation follows the original data with a normalized root mean square error of 0.3 % of short circuit current.

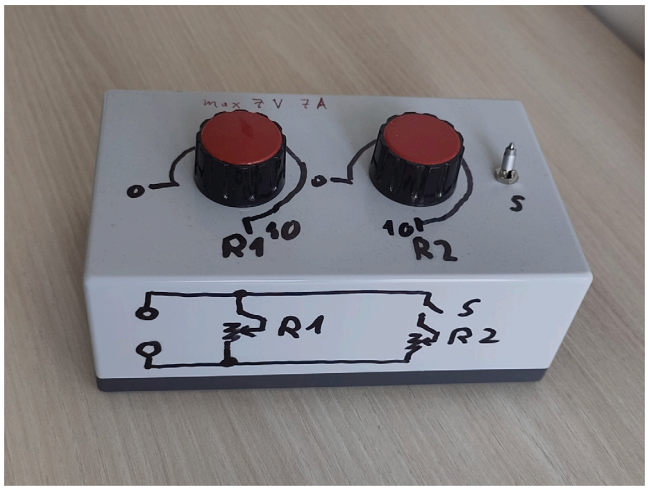

Fig. 4. Box containing two 10 Ω, 60 W potentiometers and a switch. The schematic on the front of the box depicts the working principle: by connecting or disconnecting one of the resistors which are connected in parallel results in a step increase or decrease of the total resistance.

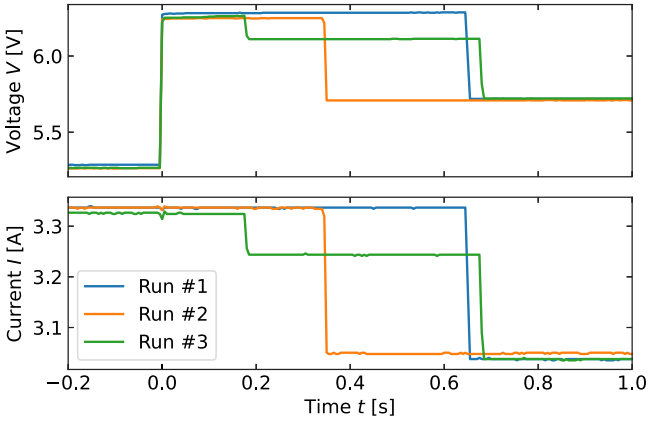

Fig. 5. Step change in ohmic load. Resistance was stepped up manually from 1.59 Ω to 1.88 Ω at Time = 0 s. Since the switching is not aligned with emulator time steps (0.5 s interval), adjustments happen at different time delays from the load step. However, all runs converge before the 1 s mark.

irradiance of the emulated device into account. Obviously, the emulator needs time series of these operating conditions to achieve this. Although it makes sense to keep them similar, sampling rates of these time series and the emulation rate can be chosen independently.

The emulator also has to use one of two more sophisticated PV models implemented in the program, both of which are based on the norm IEC60891:2021 [26]. For the parameterized model (procedure 2 in the norm) the user can choose to supply 6 model parameters and an IV-curve at standard test conditions. Alternatively the user may supply a multitude of IV-curves measured at various temperatures and fixed irradiance for bilinear interpolation of the IV-curve at the given temperature, while irradiance adjustments are handled by a proportional offset current.

In this work we based the emulated module on module "mSi0166", measured at Eugene, Oregon, from the outdoor data set published by NREL [27]. To this end we used an IEC60891:2021 procedure 2 parameterization. We used the Photo-Voltaic CuRve AnalyZEr (PVCRAZE) library to parameterize the model [28,29]. To this end we filtered the outdoor data to remove the low irradiance conditions (remove data below 500 W m^{-2}), and selected a 1000 data points to fit the IEC60891:2021 procedure 2.

Maximum output current and voltage are limited by the electrical performance of the chosen SMU. There is also a current minimum to the current limit at 50 μA imposed by the SMU while running as a voltage source. These limitations can be overcome when by using a different SCPI compatible power supply with the desired capabilities with minimal changes to the emulator code.

3. Results

3.1. Accuracy

The accuracy of the emulation was tested using the same tools used for testing of PV devices (AM1.5G class-A sun simulator from Wacom). The test was conducted with a 46-point IV-curve measured from an experimental triple junction cell using the interpolation mode of the emulator avoiding model inaccuracies. It yielded the IV-curve in Fig. 3, comparing the original measurement and its emulation. The root mean square error of the emulated current compared to the measurement when normalized to the short circuit current of the measurement is 0.3 %.

3.2. Step response

To examine the bandwidth, which is the main limitation when compared to the physical photovoltaic device, we recorded the output current and the output voltage while performing step changes in load, irradiance and temperature. The voltage was recorded using a high bandwidth oscilloscope (Keysight MSO-X 3104a) at a sampling time of 5 ms (2k samples per second). The current was measured using a current clamp with 20 kHz bandwidth (Pico Technology TA018), whose output was attached to the oscilloscope. The load for these tests consisted of two potentiometers with a resistance range of 0 Ω to 10 Ω and up to 60 W power dissipation each. Using a mechanical switch as shown in Fig. 4, this load also enabled testing of step changes of the load as shown in Fig. 5 which showed convergence within 1 s of the switching event. As this behavior results in an effective sampling rate of 1 Hz the Nyquist bandwidth is roughly 0.5 Hz.

3.3. Practical application of the emulator

Finally, we conducted two more practical tests. A 4 cm^2 proton exchange membrane (PEM) water electrolyzer cell was connected to

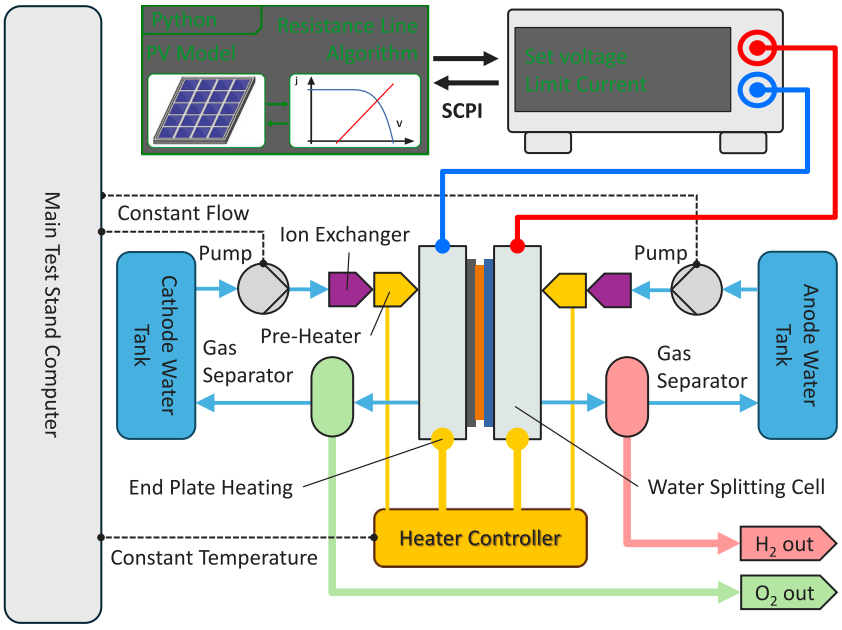

Fig. 6. Diagram of the test stand used for the practical application experiment. For this test, it maintained cell and water temperature at 80 °Celsius.

the emulator. We equipped the cell with a catalyst coated membrane (CCM) with 2.7 mg/cm^2 Ir on the anode and 0.8 mg/cm^2 Pt on the cathode side on a Nafion 117 membrane. We made the CCM in house as described previously [30]. Fig. 6 shows a diagram of the test stand used for the practical test.

We emulated two different days using data of real world operating conditions recorded during a previous project (PECSYS [31,32]), 2020-04-23 and 2020-08-18. On 2020-04-23 weather was sunny at the test site which should not be challenging with regards to the bandwidth, but made it easier to evaluate prevention of artificial ripple during practical operation Fig. 7. The ripple prevention also rejects some small scale variation in operating conditions (see inset). This is a trade-off and can be tuned by changing the size of the dead zone or setting it to zero, deactivating this feature of the emulator. Deactivation is the most reasonable choice if highest precision is required and small scale ripple is of no concern. On 2020-08-18 weather was cloudy, resulting in challenging relatively high frequency changes in irradiance, testing the emulator bandwidth under practical conditions Fig. 8.

We successfully demonstrated the practical application of the emulator with a water splitting cell in this work, but the method is applicable for variety of other electrochemical devices. We also run batteries, CO_2 reducing cells, or even combinations of both with the emulator. It is applicable to most typical electrochemical devices with the exception of devices whose IV-curves can intersect with the resistance line more than once. In the flatter region of such an IV-curve, the implementation of the resistance line algorithm shown here would not converge. For example, an electrolyzer with strong mass transport limitations could produce such a curve. However, due to the reversible voltage, such situations will usually only be caused by applying the offset voltage setting depicted in Fig. 2 and can be avoided by lowering it.

4. Discussion

The step responses show that under the chosen conditions the emulator converges from 10 % to 90 % of the step within less than 1.0 s or 2 time steps (see Fig. 5). This convergence is independent of the relative size of the step (18 % or 95 % from initial level). It is also independent of which operating condition (irradiance, temperature or load) is changed. This performance is sufficient when expecting changes in the operating

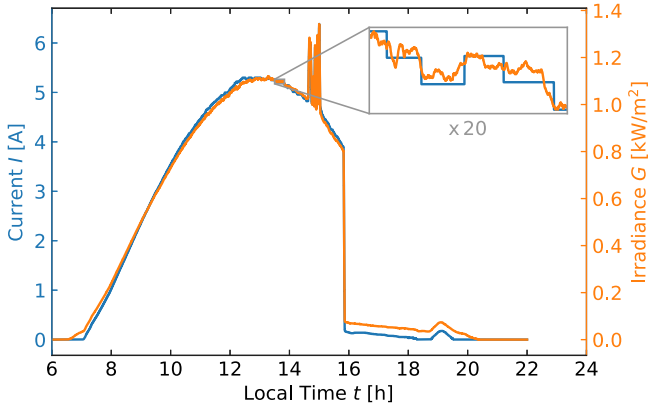

Fig. 7. Emulator output of the emulator based on the irradiance measured on the 23rd of April 2020. The day was sunny but the measurement includes two artifacts, a peak around 15 h and a sharp drop in power after that at 16 h. These are due to surrounding buildings reflecting onto and shading the tested PV system respectively. The inset is a 20 times magnified view of a 1200 s long part of the emulation. It shows how the effect of the dead zone, which is preventing small scale, short term (few seconds) oscillations.

parameters which are happening on the time scale of a few seconds or longer.

The deviation of the emulation from the recorded solar cell model is 0.3 % of short circuit current at standard testing conditions. We chose a power supply which is highly accurate in the tested range (0.035 % of full scale current). Therefore, we conservatively attribute the error to the emulation process. Since the emulation is digital (i.e. not subject to environmental influences) this accuracy is as stable over time as the power supply. If a less accurate or less stable power supply is used, its errors compound with the stated emulation error. Of course, model inaccuracies also compound with the emulation error. In [33] the authors show the parameterized model used in the emulator (labeled P2 by them) to have a root mean square error of 0.3 % without shading on a healthy PV panel.

The tests with an electrochemical load were conducted over periods of 20 h to 24 h which shows that the emulator can operate reliably and continuously over such periods. In addition, the emulation of 2020-04-23 shows no added ripple due to control action (see Fig. 7). The

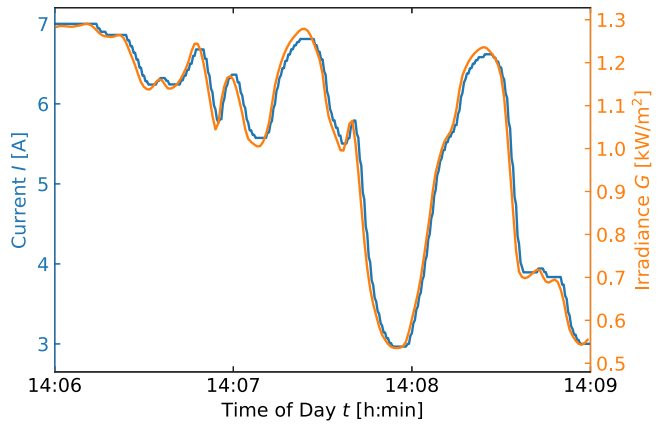

Fig. 8. Three minutes long piece of an emulation of the 18th of August 2020. Large amounts of clouds lead to numerous fast and significant increases and reductions in irradiance. The emulated current follows with a small delay of 1.1 s, approximately 2 time steps.

emulation of 2020-08-18 shows that the emulator runs slightly delayed relative to the input as expected based on the results of the step response tests (see Fig. 8). This delay of 1.1 s is much smaller than the time scale of the fastest irradiance change of about 10 s (both in terms of 10 % to 90 % rise time).

5. Conclusion

We developed a software focused implementation of an emulator for photovoltaic (PV) devices using off the shelf laboratory equipment to realize a test stand for electrochemical devices such as water electrolyzers. It is capable of high accuracy within 0.3 % of short circuit current root mean square error (I_{sc} rmse) and reliable continuous operation for at least 24 h. The parameterized PV model used to accommodate varying operating conditions has been shown by others to also reach 0.3 % I_{sc} rmse and should be the standard for future emulator developments. The slower response time of our emulator setup of about 1 s compared to a real PV device (<10 ms) has not negatively affected its application in tests with a laboratory scale PEM water electrolyzer.

Our emulator is not an improvement over state of the art in bandwidth, accuracy or similar metrics. Compared to specialized hardware, however, it is easy to implement with components which are already available at electrochemical laboratories. It only requires a computer running Python and an SCPI compatible power supply with voltage readout, current readout, voltage set and current limit functions. We believe our results help lowering the barrier of entry and will accelerate urgently needed research in PV driven electrochemistry.

CRediT authorship contribution statement

Martin Florian Seidler: Writing – review & editing, Writing – original draft, Visualization, Validation, Software, Methodology, Investigation, Formal analysis. **Bart Pieters:** Writing – review & editing, Writing – original draft, Software, Methodology. **Walter Zwaygardt:** Investigation, Data curation. **Stefan Haas:** Supervision, Funding acquisition, Conceptualization. **Oleksandr Astakhov:** Writing – review & editing, Formal analysis. **Tsvetelina Merdzhanova:** Writing – review & editing, Supervision, Formal analysis.

Declaration of competing interest

The authors declare that they have no known competing financial interests or personal relationships that could have appeared to influence the work reported in this paper.

Acknowledgments

We would like to thank Sergey Shcherbachenko (IEK-5) for proof reading, testing and applying the programs created for this work and Timon Vaas (IEK-5) for providing Python code implementing the functions given in IEC60891:2021 procedure 2. In addition, we would like to express our gratitude to Andreas Glüsen (IEK-14) for help with and feedback on the results of the practical tests.

Funding: This research was funded by the European project TELEGRAM, part of the European Union's Horizon 2020 Research and Innovation Program under grant agreement No 101006941.

Funded by the Deutsche Forschungsgemeinschaft (DFG, German Research Foundation) – 491111487.

Appendix A. Supplementary data

Supplementary material related to this article can be found online at https://doi.org/10.1016/j.jpowsour.2025.236723.

Data availability

Data will be made available on request.

References

[1] C.S. Lai, Y. Jia, L.L. Lai, Z. Xu, M.D. McCulloch, K.P. Wong, A comprehensive review on large-scale photovoltaic system with applications of electrical energy storage, Renew. Sustain. Energy Rev. 78 (2017) 439–451, http://dx.doi.org/10.1016/j.rser.2017.04.078.

[2] C. Breyer, D. Bogdanov, A. Gulagi, A. Aghahosseini, L.S. Barbosa, O. Koskinen, M. Barasa, U. Caldera, S. Afanasyeva, M. Child, J. Farfan, P. Vainikka, On the role of solar photovoltaics in global energy transition scenarios, Prog. Photovolt., Res. Appl. 25 (8) (2017) 727–745, http://dx.doi.org/10.1002/pip.2885.

[3] X. Li, L. Zhao, J. Yu, X. Liu, X. Zhang, H. Liu, W. Zhou, Water splitting: From electrode to green energy system, Nano-Micro Lett. 12 (1) (2020) 131, http://dx.doi.org/10.1007/s40820-020-00469-3.

[4] M.E. Ivanova, R. Peters, M. Müller, S. Haas, M.F. Seidler, G. Mutschke, K. Eckert, P. Röse, S. Calnan, R. Bagacki, R. Schlatmann, C. Grosselindemann, L.-A. Schäfer, N.H. Menzler, A. Weber, R. van de Krol, F. Liang, F.F. Abdi, S. Brendelberger, N. Neumann, J. Grobbel, M. Roeb, C. Sattler, I. Duran, B. Dietrich, M.E.C. Hofberger, L. Stoppel, N. Uhlenbruck, T. Wetzel, D. Rauner, A. Hecimovic, U. Fantz, N. Kulyk, J. Harting, O. Guillon, Technological pathways to produce compressed and highly pure hydrogen from solar power, Angew. Chem. Int. Ed. 62 (32) (2023) e202218850, http://dx.doi.org/10.1002/anie.202218850.

[5] G. Chehade, I. Dincer, Progress in green ammonia production as potential carbon-free fuel, Fuel 299 (2021) 120845, http://dx.doi.org/10.1016/j.fuel.2021.120845.

[6] A. Krüger, J. Andersson, S. Grönkvist, A. Cornell, Integration of water electrolysis for fossil-free steel production, Int. J. Hydrog. Energy 45 (55) (2020) 29966–29977, http://dx.doi.org/10.1016/j.ijhydene.2020.08.116.

[7] C. Ampelli, D. Giusi, M. Miceli, T. Merdzhanova, V. Smirnov, U. Chime, O. Astakhov, A.J. Martín, F.L.P. Veenstra, F.A.G. Pineda, J. González-Cobos, M. García-Tecedor, S. Giménez, W. Jaegermann, G. Centi, J. Pérez-Ramírez, J.R. Galán-Mascarós, S. Perathoner, An artificial leaf device built with earth-abundant materials for combined H2 production and storage as formate with efficiency >10%, Energy Environ. Sci. 16 (4) (2023) 1644–1661, http://dx.doi.org/10.1039/D2EE03215E.

[8] I.E.L. Stephens, K. Chan, A. Bagger, S.W. Boettcher, J. Bonin, E. Boutin, A.K. Buckley, R. Buonsanti, E.R. Cave, X. Chang, S.W. Chee, A.H.M. da Silva, P. de Luna, O. Einsle, B. Endrődi, M. Escudero-Escribano, J.V.F. de Araujo, M.C. Figueiredo, C. Hahn, K.U. Hansen, S. Haussener, S. Hunegnaw, Z. Huo, Y.J. Hwang, C. Janáky, B.S. Jayathilake, F. Jiao, Z.P. Jovanov, P. Karimi, M.T.M. Koper, K.P. Kuhl, W.H. Lee, Z. Liang, X. Liu, S. Ma, M. Ma, H.-S. Oh, M. Robert, B.R. Cuenya, J. Rossmeisl, C. Roy, M.P. Ryan, E.H. Sargent, P. Sebastián-Pascual, B. Seger, L. Steier, P. Strasser, A.S. Varela, R.E. Vos, X. Wang, B. Xu, H. Yadegari, Y. Zhou, 2022 roadmap on low temperature electrochemical CO2 reduction, J. Phys.: Energy 4 (4) (2022) 042003, http://dx.doi.org/10.1088/2515-7655/ac7823.

[9] S. Nitopi, E. Bertheussen, S.B. Scott, X. Liu, A.K. Engstfeld, S. Horch, B. Seger, I.E.L. Stephens, K. Chan, C. Hahn, J.K. Nørskov, T.F. Jaramillo, I. Chorkendorff, Progress and perspectives of electrochemical CO2 reduction on copper in aqueous electrolyte, Chem. Rev. 119 (12) (2019) 7610–7672, http://dx.doi.org/10.1021/acs.chemrev.8b00705.

[10] K. Sadeghi, Y. Jeon, J. Seo, Roadmap to the sustainable synthesis of polymers: From the perspective of CO2 upcycling, Prog. Mater. Sci. 135 (2023) 101103, http://dx.doi.org/10.1016/j.pmatsci.2023.101103.
[11] R. Casebolt, K. Levine, J. Suntivich, T. Hanrath, Pulse check: Potential opportunities in pulsed electrochemical CO2 reduction, Joule 5 (8) (2021) 1987–2026, http://dx.doi.org/10.1016/j.joule.2021.05.014.
[12] S.M. Alia, S. Stariha, R.L. Borup, Electrolyzer durability at low catalyst loading and with dynamic operation, J. Electrochem. Soc. 166 (15) (2019) F1164, http://dx.doi.org/10.1149/2.0231915jes.
[13] H. Kojima, K. Nagasawa, N. Todoroki, Y. Ito, T. Matsui, R. Nakajima, Influence of renewable energy power fluctuations on water electrolysis for green hydrogen production, Int. J. Hydrog. Energy 48 (12) (2023) 4572–4593, http://dx.doi.org/10.1016/j.ijhydene.2022.11.018.
[14] A.Z. Tomić, I. Pivac, F. Barbir, A review of testing procedures for proton exchange membrane electrolyzer degradation, J. Power Sources 557 (2023) 232569, http://dx.doi.org/10.1016/j.jpowsour.2022.232569.
[15] J.P. Ram, H. Manghani, D.S. Pillai, T.S. Babu, M. Miyatake, N. Rajasekar, Analysis on solar PV emulators: A review, Renew. Sustain. Energy Rev. 81 (2018) 149–160, http://dx.doi.org/10.1016/j.rser.2017.07.039.
[16] A. Xenophontos, J. Rarey, A. Trombetta, A.M. Bazzi, A flexible low-cost photovoltaic solar panel emulation platform, in: 2014 Power and Energy Conference at Illinois, PECI, 2014, pp. 1–6, http://dx.doi.org/10.1109/PECI.2014.6804542.
[17] M. Power, Solar Emulation and Inverter Testing, 2023, https://magna-power.com/de/learn/application/solar-emulation-inverter-testing.
[18] Chroma USA, Solar array simulator DC power supply, 2023, https://www.chromausa.com/product/solar-array-simulator/.
[19] BeXema, PV-emulator: BeXema, 2023, https://bexema.com/de/produkte/hochvolt-emulatoren/pv-emulator/.
[20] Tektronix, 2460 SourceMeter SMU Instrument Datasheet, Datasheet, Tektronix, 2023, p. 14.
[21] F. Bode, J. Pieper, Standard Commands for Programmable Instruments (SCPI), 1999.
[22] National Instruments, NI-VISA-download, 2023, https://www.ni.com/de/support/downloads/drivers/download.ni-visa.html.
[23] M. Pravettoni, D. Poh, J.P. Singh, J.W. Ho, K. Nakayashiki, The effect of capacitance on high-efficiency photovoltaic modules: A review of testing methods and related uncertainties, J. Phys. D: Appl. Phys. 54 (19) (2021) 193001, http://dx.doi.org/10.1088/1361-6463/abe574.
[24] M. Olama, J. Dong, I. Sharma, Y. Xue, T. Kuruganti, Frequency analysis of solar PV power to enable optimal building load control, Energies 13 (18) (2020) 4593, http://dx.doi.org/10.3390/en13184593.
[25] P. Virtanen, R. Gommers, T.E. Oliphant, M. Haberland, T. Reddy, D. Cournapeau, E. Burovski, P. Peterson, W. Weckesser, J. Bright, S.J. van der Walt, M. Brett, J. Wilson, K.J. Millman, N. Mayorov, A.R.J. Nelson, E. Jones, R. Kern, E. Larson, C.J. Carey, İ. Polat, Y. Feng, E.W. Moore, J. VanderPlas, D. Laxalde, J. Perktold, R. Cimrman, I. Henriksen, E.A. Quintero, C.R. Harris, A.M. Archibald, A.H. Ribeiro, F. Pedregosa, P. van Mulbregt, SciPy 1.0: fundamental algorithms for scientific computing in Python, Nature Methods 17 (3) (2020) 261–272, http://dx.doi.org/10.1038/s41592-019-0686-2.
[26] I.E. Commission, IEC 60891:2021 Photovoltaic Devices - Procedures for Temperature and Irradiance Corrections to Measured I-V Characteristics, IEC, 2021.
[27] B. Marion, A. Anderberg, C. Deline, M. Muller, G. Perrin, J. Rodriguez, S. Rummel, T. Silverman, F. Vignola, S. Barkaszi, Data for Validating Models for PV Module Performance, Technical Report, EMN-DURMAT (EMN-DuraMAT); National Renewable Energy Lab. (NREL), Golden, CO (United States), 2021, http://dx.doi.org/10.21948/1811521.
[28] B. Pieters, Extended solar cell parameters - general purpose descriptive I/V parameters for solar cells, Theory Appl. Categ. (2023) http://dx.doi.org/10.22541/au.169460479.90599786/v1.
[29] B.E. Pieters, PV-Craze, 2022, https://github.com/IEK-5/PV-CRAZE.
[30] C. Rakousky, G.P. Keeley, K. Wippermann, M. Carmo, D. Stolten, The stability challenge on the pathway to high-current-density polymer electrolyte membrane water electrolyzers, Electrochim. Acta 278 (2018) 324–331, http://dx.doi.org/10.1016/j.electacta.2018.04.154, URL https://www.sciencedirect.com/science/article/pii/S0013468618309150.
[31] S. Calnan, R. Bagacki, F. Bao, I. Dorbandt, E. Kemppainen, C. Schary, R. Schlatmann, M. Leonardi, S.A. Lombardo, R.G. Milazzo, S.M.S. Privitera, F. Bizzarri, C. Connelli, D. Consoli, C. Gerardi, P. Zani, M. Carmo, S. Haas, M. Lee, M. Mueller, W. Zwaygardt, J. Oscarsson, L. Stolt, M. Edoff, T. Edvinsson, I.B. Pehlivan, Development of various photovoltaic-driven water electrolysis technologies for green solar hydrogen generation, Sol. RRL 6 (5) (2022) 2100479, http://dx.doi.org/10.1002/solr.202100479.
[32] M. Müller, W. Zwaygardt, E. Rauls, M. Hehemann, S. Haas, L. Stolt, H. Janssen, M. Carmo, Characteristics of a new polymer electrolyte electrolysis technique with only cathodic media supply coupled to a photovoltaic panel, Energies 12 (21) (2019) 4150, http://dx.doi.org/10.3390/en12214150.
[33] B. Li, D. Diallo, A. Migan-Dubois, C. Delpha, Performance evaluation of IEC 60891:2021 procedures for correcting I–V curves of photovoltaic modules under healthy and faulty conditions, Prog. Photovolt., Res. Appl. 31 (5) (2023) 474–493, http://dx.doi.org/10.1002/pip.3652.